Synthesis of fluorescent core-shell nanomaterials and strategies to generate white light

Amandeep Singh, Ramanjot Kaur, O. P. Pandey, Xueyong Wei, and Manoj Sharma

Synthesis of fluorescent core-shell nanomaterials and strategies to generate white light

Amandeep Singh,[1] Ramanjot Kaur,[1] O. P. Pandey,[2] Xueyong Wei,[3] and Manoj Sharma[1,4,a)]

[1]*Department of Nanotechnology, Sri Guru Granth Sahib World University, Fatehgarh Sahib, India*
[2]*School of Physics and Materials Science, Thapar University, Patiala 147004, India*
[3]*State Key Laboratory for Manufacturing System Engineering, Xi'an Jiaotong University, 710049 Xi'an, China*
[4]*UNAM–Institute of Materials Science and Nanotechnology, Bilkent University, Ankara 06800, Turkey*

In this work, cadmium free core-shell ZnS:X/ZnS (X = Mn, Cu) nanoparticles have been synthesized and used for white light generation. First, the doping concentration of Manganese (Mn) was varied from 1% to 4% to optimize the dopant related emission and its optimal value was found to be 1%. Then, ZnS shell was grown over ZnS:Mn(1%) core to passivate the surface defects. Similarly, the optimal concentration of Copper (Cu) was found to be 0.8% in the range varied from 0.6% to 1.2%. In order to obtain an emission in the whole visible spectrum, dual doping of Mn and Cu was done in the core and the shell, respectively. A solid-solid mixing in different ratios of separately doped quantum dots (QDs) emitting in the blue green and the orange region was performed. Results show that the optimum mixture of QDs excited at 300 nm gives Commission Internationale del'Éclairage color coordinates of (0.35, 0.36), high color rendering index of 88, and correlated color temperature of 4704 K with minimum self-absorption. © 2015 AIP Publishing LLC.
[http://dx.doi.org/10.1063/1.4927482]

I. INTRODUCTION

In the last two decades, transition metal doped semiconductor nanocrystals have been widely investigated because of their tunable emission spanning over the whole visible region.[1–12] Among them, Mn and Cu-doped semiconductor nanocrystals were of great importance as Mn provides a short-range emission and Cu results in a host bandgap-dependent wide range tunable emission.[11,12] Therefore, their tunable PL emissions can be used to generate white light. The quality of a white light source is usually evaluated by three performance parameters: CIE, CRI, and CCT.[10] In CIE (Commission Internationale del'Éclairage) color diagram, a perfect white light is produced at a point (x, y) = (0.33, 0.33).[10] Color rendering index (CRI) is the measure of color rendition of the white light source. The best color rendition is expressed with a CRI of 100, whereas the CRI of the poorest color rendition is expressed as −100. Furthermore, the quality of a light source is also evaluated in terms of the correlated color temperature (CCT), which illustrates the temperature of a closest Planckian black-body radiator to the operating point on the chromaticity diagram.[10]

There are various methods to achieve white-light emission. The first one is the multichip white LEDs which consist of red, blue, and green emitting chips and thus shows a good CRI. However, these types of LEDs are costly and have complex electronic system to account for different degradation rate of different types of chips. The second type is the ZnSe based white LEDs which have two emission bands: blue from the active layer of ZnSe and yellow from the ZnSe substrate.[10] However, these types of LEDs have lower emission efficiency and shorter lifetime comparatively. The third type is the single chip white LEDs that comprises blue InGaN chip and yellow emitting yttrium aluminum garnet (YAG) phosphor.[10] The YAG doped with cerium (YAG: Ce) phosphor is most widely used in these types of LEDs. However, this leads to a low CRI value as the YAG: Ce phosphor lacks emission in the red region. The application of QDs as down converter in white LEDs has been employed to improve the CRI values.[10,11] Therefore, white light emission can be obtained by mixing different color emitting QDs together, but it may lead to a poor photometric performance and undesirable changes in CIE coordinates.[12,13] This is mainly due to self-absorption of QDs and an improper mixing of all the emissions will lead to a poor white light generation. To address this problem, a single system emitting different colors was achieved by synthesizing doped QDs in solution having different dopants. However, the host matrix tends to expel the dopant ions from the internal crystal lattice to the surface in sort of self-purification process.[14] Hence doping is difficult even in most favorable cases of dopants having same charge and ionic radius as that of host. Nag and Sharma[15] reported white light generation from Mn doped CdS nanocrystals and addressed the problem of self-absorption in nanocrystals caused by the large stoke shift in absorption and emission spectra. However, cadmium is a highly toxic material and hence hazardous to the environment. Also covering whole visible spectrum for perfect white light generation from single dopant ions is not possible. Another approach adopted to address this problem was co-doping. Mostly, it has been observed that during co-doping the emission from one of the dopants is suppressed by the other due to the interaction between the dopants. There are

a)Author to whom correspondence should be addressed. Electronic addresses: manojnarad@gmail.com and manojsharma@bilkent.edu.tr

several reports describing the synthesis of semiconductor nanocrystals (NCs) with white light emission such as CdSe NCs, alloyed $Zn_xCd_{1-x}Se$ QDs, ZnS:Pb, and ZnS incorporated into porous silicon, Mn, Cu co-doped ZnSe, and ZnS:Mn QDs.[16–21]

It is expected that a high quality white light emission from a mixture of differently doped QDs can be achieved. The problems associated with a simple mixing are re-absorption of the emitted photon by other QDs, excitation of mixture of QDs at different wavelengths, and out of phase emission of different QDs. These will lead to a poor CRI and an unwanted change in CIE as redundant color hues will be present in output.[22] Herein, we report the synthesis of highly luminescent core/shell ZnS:X/ZnS (X = Mn, Cu) NPs and nearly perfect white light emission from a mixture of differently doped QDs. First, ZnS:Mn and ZnS:Cu cores were synthesized and the optimal doping concentrations were experimentally worked out. Then ZnS shell was grown over the core to passivate the surface defects. The advantage of inorganic shell is experimentally verified by increase in overall emission and quantum efficiency. The core-shell QDs with dual doping (doping in core and shell, respectively) strategies were tried to cover the whole visible spectrum. However, the co-doping was not achievable due to mild conditions of synthesis. Solid–solid mixing of two separately doped core shell QDs was instead studied in order to span the complete visible spectrum. Finally, superior white light performance having CIE color coordinates of (0.35,0.36), high CRI of 88 and CCT of 4704 K with minimum self-absorption was achieved by tuning the relative concentration of the highly luminescent QDs and using a single wavelength excitation source.

II. EXPERIMENTAL DETAILS

A. Materials and chemicals

Analytically pure zinc acetate ($Zn(CH_3COO)_2$), manganese acetate tetra-hydrate ($Mn(CH_3COO)_2 \cdot 4H_2O$), sodium sulphide nona-hydrate ($Na_2S \cdot 9H_2O$), and copper acetate ($Cu(CH_3COO)_2$) were used as-received from Sigma Aldrich. Other chemical reagents were used without further purification.

B. Experimental procedures

The bottom up wet chemical synthesis route was used to synthesize orange and green emitting core shell NPs.[23] The Zinc Sulphide (ZnS) core was doped with Manganese (Mn) and Copper (Cu) separately. The shell of ZnS was formed over the doped core. Further efforts were done to synthesize dual doped NPs with Mn doped in core and Cu doped in shell under mild synthesis environment. The experimental details are given below.

C. Synthesis of ZnS:X core (X = Mn, Cu)

The aqueous stock solution was prepared as follows: 0.5 M solution of zinc precursor was prepared by adding 9.17 g of zinc acetate in 100 ml double distilled water. Then, the amount of zinc acetate was varied and manganese acetate

(or copper acetate) was added to the solution, to vary the doping concentration from 1.0 to 4.0% at. for Mn (or 0.6 to 1.2% at. for Cu). Thus, zinc precursor solution with different amount of dopants was vigorously stirred at a constant temperature of 80 °C. 40 ml of 0.5 M thioglycerol (TG) solution was prepared by mixing 1730 μl TG in 40 ml of the double distilled water. An appropriate amount of 0.5 M Sodium Sulphide (Na_2S) was prepared as a reducing agent.

Sample preparation: 20 ml of buffer solution of zinc acetate doped with Mn (or Cu) was taken in a flask and 40 ml solution of capping agent (TG) was added to it. The above solution was stirred for 5 min at 80 °C. 0.5 M Sodium Sulphide (Na_2S) was added to above mixture drop-wise and temperature was reduced to 70 °C, while stirring was continued. Finally, the above mixture was stirred for 12 h with a slow increase in temperature to 80 °C. The solid powders of ZnS:Mn/Cu core NPs were obtained after adding excess ethanol to the solution followed by drying in vacuum.

D. Synthesis of ZnS:X/ZnS core-shell NPs (X = Mn, Cu)

Zinc acetate and TG stock solution of 0.5 M concentration was prepared by adding an appropriate amount of zinc acetate and TG into aqueous solution [labeled as solution A]. The powder of NPs formed in Section II C was dissolved in DI water so that final concentration of solution is 0.05 M. 20 ml stock solution was added into the NPs solution drop wise and the mixture was stirred for 6 h at the temperature of 80 °C. Finally, ZnS:X/ZnS core shell NPs were obtained after adding excess ethanol and drying in vacuum.

E. Synthesis of dual doped NPs (ZnS:Mn/ZnS:Cu)

The synthesis of core doped with Mn was done in a similar way as did in step one (Section II C). The powder of Mn doped NPs formed in Section II C was dissolved in DI water, so that final concentration of solution is 0.05 M. This sample is used as core for dual doped synthesis. For Cu doped shell growth, the aqueous stock solution (0.1 M) of zinc acetate and copper acetate were prepared, under vigorously stirring and maintaining a constant temperature of 80 °C. The doping concentration of Cu was 0.8% (at.). Then, 0.1 M TG solution was added and labeled as solution B. Both the solutions (ZnS:Mn core and solution B) were mixed and stirred continuously for 6 h at 80 °C, so that (ZnS:Cu) shell grows over the core (ZnS:Mn) NPs. The dual doped material ZnS:Mn/ZnS:Cu was obtained after adding excess ethanol and drying in vacuum.

F. Formation of mixture of QDs

The powder samples of both QDs (ZnS:Mn/ZnS and ZnS:Cu/ZnS) were used to make equal concentration (0.01M) of aqueous QDs colloidal solution. Seventeen samples were prepared with various ratios of both the solutions (Table S1, Ref. 24) to study the effect of different QDs on the overall luminescence property.

Thus, by following the above procedure these samples were prepared: ZnS: Mn core NPs, ZnS:Mn/ZnS core-shell

NPs, ZnS: Cu core NPs, ZnS:Cu/ZnS core-shell NPs, ZnS:Mn/ZnS:Cu(dual doped) coreshell NPs, and ZnS:Mn/ZnS + ZnS:Cu/ZnS mixed QDs. The schematic of synthesized NPs showing white-light is shown in Figure 1.

G. Instrumentation and measurements

The NPs were characterized by X-ray diffraction (XRD) using Panalytical X'pert Pro MPD with Cu-Kα radiation. HRTEM images of synthesized samples were recorded using analytical transmission electron microscope (Model JEM-2100F). For HRTEM study, a drop of the QD solution dispersed in methanol was dropped on a carbon-coated Cu grid. Methanol was evaporated to leave QDs on the grid. Optical absorption spectra of the ZnS NPs were recorded with a double beam UV-Visible spectrophotometer (Model: Shimadzu/ UV 2600) in the range of 200–800 nm. Photoluminescence studies and calculation of CIE color coordinates of all the prepared samples were done with an Edinburgh Instruments FS920 spectrometer equipped with a 450W Xenon Arc Lamp and a cooled single photon counting photomultiplier (Hamamatsu R2658P). For PL (excitation and emission) studies, ZnS NPs in equal concentration were used. Absolute quantum yields (QYs) were measured using an integrating sphere and a Xenon lamp as excitation source.

III. RESULTS AND DISCUSSION

A. Structural studies

X-ray diffraction pattern of ZnS doped core and core-shell NPs shows three broad peaks corresponding to the (111), (220), and (311) planes of FCC ZnS structure (Figure S1, Ref. 24). The peaks observed in the XRD pattern match well with those of the β-ZnS (cubic) reported in the ICDD Powder Diffraction files (File. No. 77–2100). Crystallite size of ZnS NPs was calculated by Scherer's equation which is in the range of 4.0–5.0 nm for core and core-shell QDs. Broadening of the XRD peaks for capped samples indicates the formation of ZnS nanocrystals. The nanocrystals have
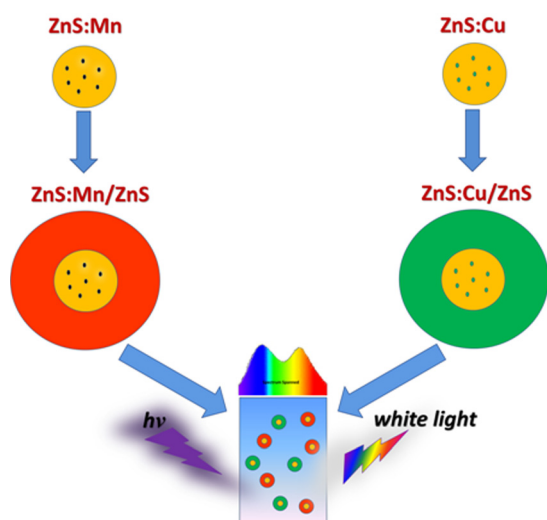
lesser lattice planes compared to bulk which contributes to the broadening of peaks in the diffraction pattern. There is a little shift in diffraction peaks to larger angles as the shell is formed. No characteristic peaks of impurity phases are observed in the XRD pattern, indicating the high purity of the final products.

Figure 2(a) shows the high-resolution TEM (HRTEM) image of ZnS:Mn/ZnS core shell NPs (scale bar: 5 nm). The inset (b) shows magnified image of single NP. Since the core and the shell of the QDs had similar electron densities and lattice parameters, but doping in core creates slight image contrast that distinguishes the shell and the core. The high crystallinity of the prepared NPs is justified since the distance (0.317 nm) between the adjacent lattice fringes is the interplanar distance of ZnS ⟨111⟩ plane, which is in a good agreement with the ⟨111⟩ d-spacing value of 0.312 nm reported in literature.[25] The high crystallinity of NPs depends upon the rate of reaction. The reducing agent mentioned in Section II C was added drop-wise and at same time temperature was reduced to slow down the rate of reaction which promotes narrow size distribution. Figure 2(c) shows the HRTEM image of ZnS:Cu/ZnS at scale bar 10 nm. Inset figure shows magnified image of single NP, which clearly shows the lattice planes. Figure 2(d) shows the HRTEM image of ZnS:Cu/ZnS at scale bar 5 nm. From TEM measurements, it is observed that all synthesized QDs are having average size of 5–6 nm.

B. Absorption studies

Optical studies were performed by measuring the absorption of the samples in the wavelength range of 200–800 nm. Figure 3(a) shows absorbance versus wavelength (λ) graph for ZnS:Mn/ZnS core shell QDs. The absorption spectrum of

FIG. 1. Schematic of formation of doped core-shell QDs and white light generation.
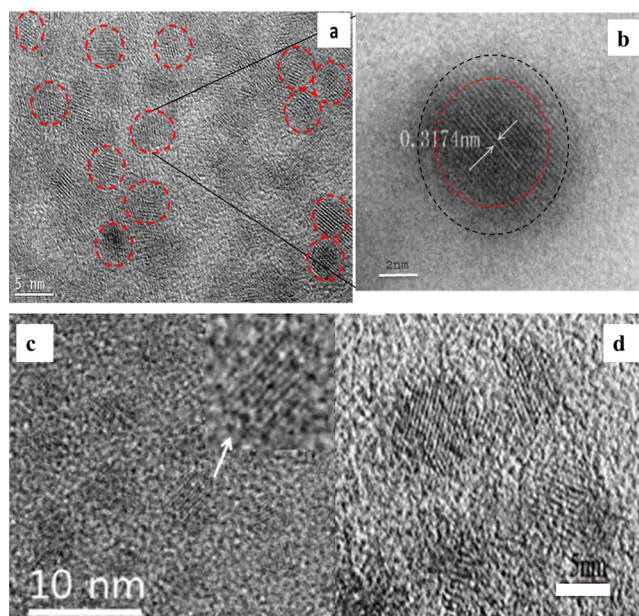

FIG. 2. (a) The High-Resolution TEM (HRTEM) image of ZnS:Mn/ZnS core shell NPs (scale bar: 5 nm). The inset (b) shows magnified image of single NP, (c) the HRTEM image of ZnS:Cu/ZnS at scale bar 10 nm. Inset figure shows magnified image of single NP, (d) the HRTEM image of ZnS:Cu/ZnS at scale bar 5 nm.

QDs shows absorption edge at 300 nm. Thus, the absorption edge has fairly blue shifted as compared to that of the bulk (334 nm). The absorption coefficients (α) were obtained in the region of strong absorption by calculating the transmittance data using Manifacier model.[26] To determine the band gap of synthesized QDs, the fundamental absorption which corresponds to the transition from valence band to the conduction band was used. The relation between absorption coefficient (α) and incident photon energy (hν) can be written as[26]

$$\alpha = A(h\nu - E_g)^n / h\nu, \qquad (1)$$

where A is constant, E_g is the band gap of the material, and the exponent n depends on the type of transition. The value of n is 1/2, 2, 3/2, and 3 corresponding to the allowed direct, allowed indirect, forbidden direct, and forbidden indirect transitions, respectively. The exact value of band gap can be determined by extrapolating the straight line portion of the $(\alpha h\nu)^{1/n}$ versus hν axis (Fig. S2, Ref. 24). The band gap value decreases with increasing doping concentration. This is due to the change of particle size which increases with increasing doping concentration of Mn ion. Similar results were reported by Kole *et al.*[12] Further for all synthesized samples band gap is larger than the band gap of corresponding bulk ZnS (3.6 eV), which is due to the strong quantum confinement effects. The formation of shell over the core leads to a small red shift (5–10 nm) in UV-Visible absorption spectra wavelength compared to the uncoated core. A shift of 8 nm was observed in case of ZnS:Cu (core) vs. ZnS:Cu/ZnS (core-shell) QDs, as shown in Figure 3(b). In the case of Mn doped core vs. Core-shell QDs the shift was 10 nm (Figure 3(c)).

C. Luminescence studies

Figure 4(a) shows emission mapping of ZnS:Mn/ZnS core shell NPs. The excitation wavelength varies from 280 nm to 340 nm, with step size of 10 nm. The excitation wavelength of sample prepared is 300 nm since at this particular excitation, the emission from sample is maximum. This is also visible from the excitation scan of sample corresponding to dopant emission at 590 nm (Figure 4(b)). Earlier we have shown tunable emission in the inorganic-organic hybrid NPs by FRET (Foster Resonance Energy Transfer) mechanism.[23,27] CIE chromaticity coordinates shifts from (0.27, 0.20) to (0.34, 0.27) for chitosan capped and Mn doped ZnS QDs by suitably tuning excitation energy in the higher and lower ultra-violet (UV) range. These materials can be used for bio-sensing applications, but the photometric properties of these NPs were not superior. For the opto-electronic and lighting application, the emission must be tuned to achieve superior photometric properties like CRI (better than 85), CIE close to white light (0.33, 0.33). Quan *et al.*[21] reported a multi-color tuning of Mn doped ZnS colloidal nanocrystals under single excitation wavelength. White emission was realized for Mn^{2+} doped ZnS nanocrystals, with a good CIE co-ordinate (0.31, 0.30). However, they did not report the CRI values, which indicate the color quality.

To improve the color quality, the output in visible region should be tuned, especially in deep green to yellow region of spectrum, thereby addressing the green window problem.[10] Figure 4(c) shows the dependence of luminescence intensity on the doping concentration of Mn. First, the doping concentration of Mn in core of core-shell system was varied from 1 to 4% (at.) to optimize the emission. It was observed that the characteristic emission due to Mn doping was found to be
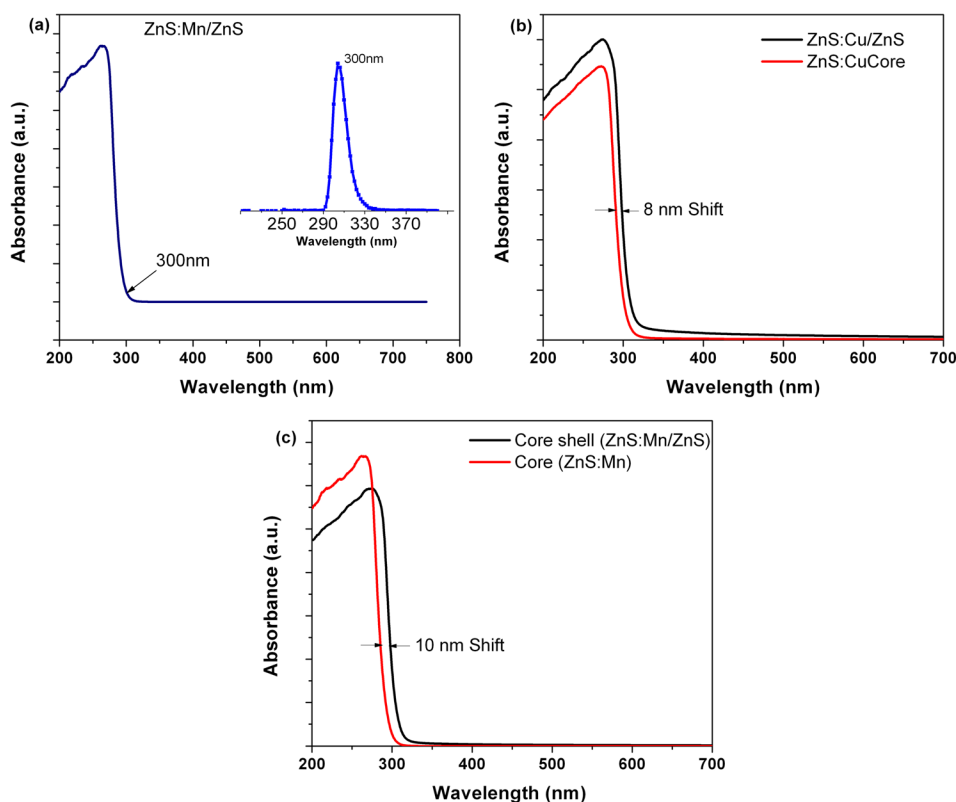

FIG. 3. (a) Absorption spectrum of ZnS:Mn/ZnS core shell QDs, with absorption edge at 300 nm. The Inset is the excitation scan of sample which shows peak at same wavelength. (b) Shift in UV spectrum due to formation of shell. (c) Absorption spectrum of ZnS:Cu/ZnS core-shell QDs.
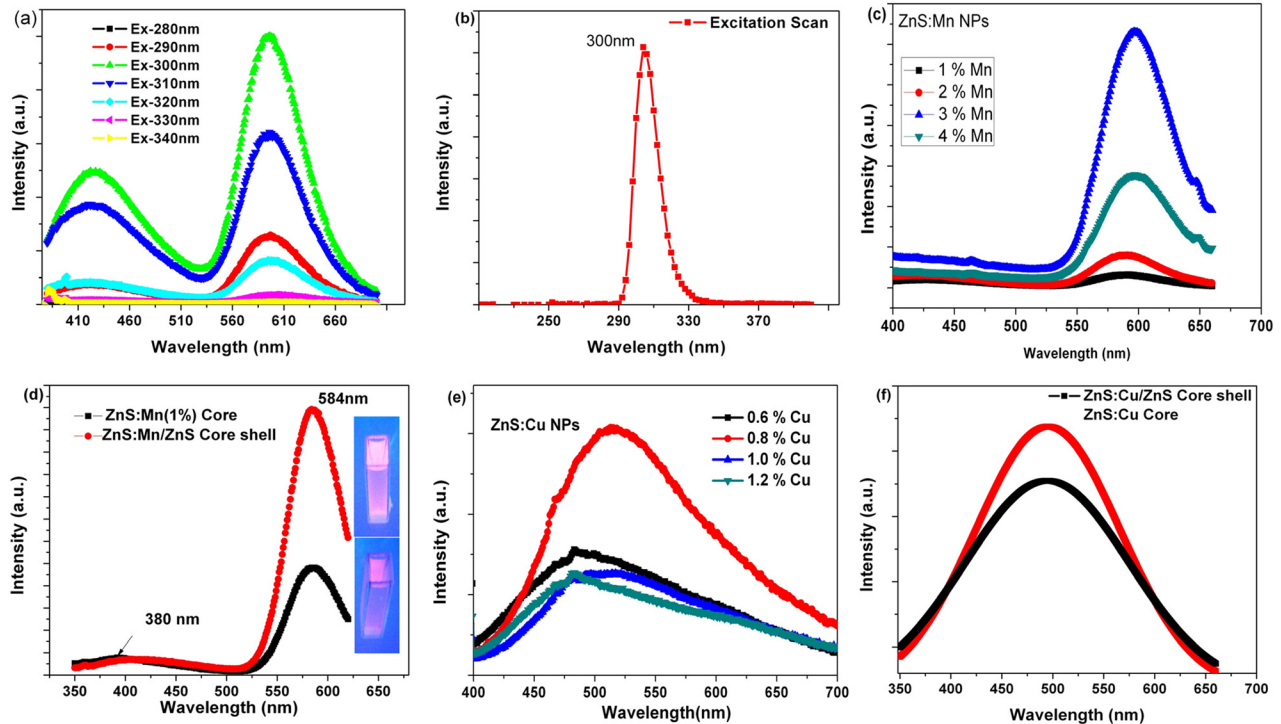
FIG. 4. (a) Photo luminescence emission spectra of ZnS:Mn/ZnS core shell NPs at different excitation wavelength, (b) excitation spectra of ZnS:Mn/ZnS core shell NPs corresponding to dopant emission at 590 nm, (c) variation of luminescence of ZnS: Mn with doping concentration, (d) PL of core and core-shell ZnS NPs with 1% (at. wt.) doping of Mn, (e) variation of luminescence of ZnS: Cu NPs with different Cu concentration, (f) PL spectrum of core and core-shell NPs with 0.8% (at. wt.) doping of Cu.

dependent on doping concentration of Mn in ZnS. The optimum concentration was found to be near 1% (at.). The similar concentration was quoted by Kole *et al.*[12] It has been observed that as the doping concentration increases above 1%, the luminescence intensity decreases. Figure 4(d) shows emission spectra of core (ZnS:Mn) vs. core-shell (ZnS:Mn/ZnS) QDs at 300 nm excitation wavelength. The inset shows bright colloidal solution of QDs under UV illumination. The core has two characteristic emissions, one related to defect/vacancy related emission of host ZnS material close to 400 nm and other is dopant related emission ($^4T_1 \rightarrow {}^6A_1$) of Mn^{2+} close to 590 nm.[23,28,29] It is because the NPs have high surface to volume ratio that surface defects can quench the emission by providing the alternative path of nonradiative relaxation. The formation of the shell (inorganic capping) over the core not only passivates these defects but at the same time can also satisfy cationic and anionic dangling bonds, thereby blocking the alternative path for nonradiative transition. The ratio of emission intensity from dopant (DOP) vs defect (DF) in case of core QDs is IDOP/DF(C) = 6.07, while in case of core-shell QDs, IDOP/DF (CS) is 15.07 (Figure 4(d)). Thus, the relative increase of 59.7% has been observed in core/shell NPs. These results imply that the passivation of surface defects by shell significantly enhances the dopant related emission in comparison with defects related emission.

Similarly, the doping concentration of Cu in ZnS: Cu NPs was varied from 0.6 to 1.2% (at.) to find out the optimized emission from the samples (Figure 4(e)). It has been

reported earlier that the PL emission peak around 434 nm for undoped ZnS is attributed to the sulfur vacancies and ZnS QDs will have a large number of sulfur vacancies (VS) during precipitation at low concentrations of sulfide ions.[27,30,31] Bearing a charge of 2+, the VS sites can effectively trap excited electrons from the conduction band and act as a doubly ionized donor by forming a shallow energy level below the conduction band (CB) edge. Subsequent electron–hole (e–h) recombination at the valence band lead to blue emissions, referred to as "self-activated" emission in nanosized ZnS.[30] As shown in Figure 4(e), broad emission peak from 400 to 600 nm is observed which shows contribution from sulfur vacancies and dopant states. In addition, there is a small variation in peak position (red shift) with increased Cu doping. The maximum emission intensity was obtained at 0.8% doping of Cu in ZnS. The reason behind the variation in peak can be explained by the luminescence mechanism of ZnS:Cu. The doped Cu ions form deep energy levels between valence band (VB) and CB of ZnS. As the electrons absorb external energy, they are excited from VB to CB and go to the defect levels formed by Cu ions. Thus, the electrons will recombine with holes in the VB and the holes in the Cu energy levels from shallow sulfur vacancies by radiative transitions. So the emission is possible from both ZnS (defect states/sulfur vacancies) and Cu at the same time having relative contributions variable with different doping concentrations. The energy levels of Cu ions vary with doping concentration. Thus, slightly different emission wavelengths can be obtained by varying the concentration of Cu ions.

From the luminescence mechanism, it is clear that Cu acts as optically active luminescence centers in ZnS NPs because they substitute Zn in the lattice and the luminescence from ZnS:Cu depends on Cu concentration. Similar variation in emission spectra has been reported earlier with variation in Cu doping in host ZnS.[30,31] Figure 4(f) shows the optimized luminescence output of Cu doped core and core-shell QDs. It is clear that optimum doping concentration is 0.8% (at.) and this was used for synthesis of core-shell QDs. The enhancement in the overall emission for ZnS:Cu/ZnS core-shell QD in comparison to the core was observed. This improvement is due to the passivation of surface defects at the shell which have more probability for non-radiative decay. Figure 4(e) shows broad emission peaks centered at 530 nm spanning blue green region. Absolute QYs of Mn doped and Cu doped QDs were measured using an integrating sphere and a Xenon lamp as excitation source. Mn doped core and coreshell QDs have shown absolute QY from 8.0% to 14.1% and Cu doped core and core-shell QDs have shown absolute QY of 1.8%–4.8%, respectively.

Figure 5(a) shows graphical illustration of spectrum that can be generated using phosphor QDs, the inset (right) shows spectrum generated by Compact Florescent Lamp (CFL). It is clear that the emission in visible spectrum generated by CFL bulb does not span the region entirely, resulting in poor photometric properties. The inset (left in figure) shows exemplary spectrum of existing LEDs with green window problem.[10] Therefore, there are two objectives to be fulfilled, one to get better output in the region of visible spectrum and at the same time achieving high CRI (>85) from QD phosphors. This can be achieved in two ways: First way is by synthesizing core-shell (or multi core-shell) system to generate white light. In such systems white light is obtained by combining emission from core and shell structure (Figure 5(b)). Second way is to synthesize a mixture of obtained independently radiating QDs (Figure 5(c)).

Assuming the mixture of QDs to be independent radiator, then the resultant emission from both QDs is just a superposition of individual QDs. The generalized formula for emission can be written as

$$I_R = I_{QD(1)} + I_{QD(2)}. \tag{2}$$

Figure 5(d) shows the resultant output, according to Eq. (2). The emission from individual QDs lies in visible region, while the excitation of both QDs lies in UV (300 nm) region.
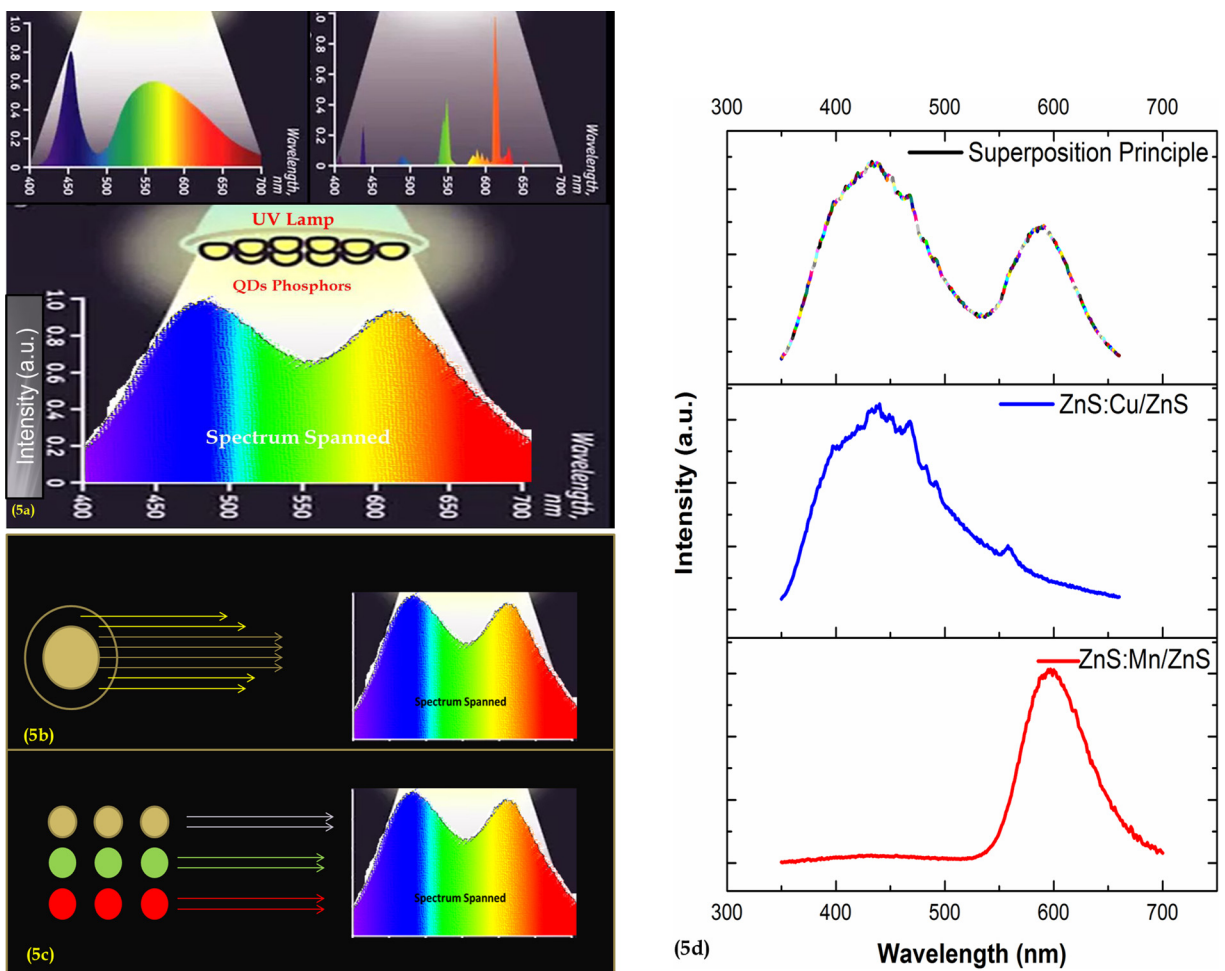

FIG. 5. (a) Emission spectrum generated by mixture of QDs. Inset (right) shows spectrum generated by CFL bulb. Inset (left) shows spectrum of available LEDs, with green window problem, (b) illustrates generation of white light by combining emission from core and shell, (c) illustrates generation of white light by combining emission from independently radiating mixture of quantum dots, (d) theoretically predicted graph according to principle of superposition of solid-solid mixture of Cu doped and Mn doped core shell NPs.
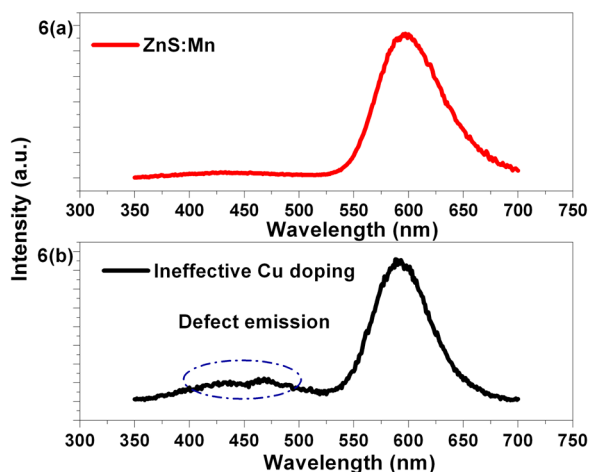
FIG. 6. PL spectrum of (a) ZnS: Mn core and (b) dual doped ZnS:Mn/ZnS:Cu QDs.

Therefore, it is impossible that emission from one type of QD to be absorbed by the other type, leading to minimize the problem of self-absorption.

To span the whole visible spectrum having good CRI, dual doped materials with Mn in the core and Cu in the shell (ZnS:Mn/ZnS:Cu) were tested. Since Mn doped core-shell QDs give bright emission in orange region and Cu doped core-shell QDs emit in blue green region individually. In order to get better CRI index and lower CCT (Correlated Color Temperature), the emission in orange red region must be increased in comparison to rest of the region, as observed from the experiments [Table SI, Ref. 24]. The main reason for Mn doping in the core instead of the shell is that the output around 550–650 nm gives better CRI index and low CCT temperature. Mn ions related emission is better in the core in comparison with shell as the core is better passivated. Recently, Hazarika *et al.*[32] have reported tuning of Mn emission over the entire visible spectral range at an ensemble scale by controlling the strain generated due to an epitaxial growth of a semiconductor shell over a semiconductor core. Figure 6(a) shows core ZnS:Mn QDs, showing the dopant related strong emission in orange region. However, it was observed that the Cu doped in the shell does not give the desired emission (Figure 6(b)). The emission of Cu in blue green region was very less compared with that of Mn dopant. The percentage ratio of dopant emission of Mn vs Cu comes out to 64.43%. This is because the Cu dopant is in the shell, which may have defect states (higher in comparison with the

Mn doped core) that are not passivated, thereby increasing the non radiative path ways for blue green emission. Thus, there will be always a problem with the dopant ions exposed to the environment.[33,34] The multishell structures have been reported earlier, where these materials have large lattice mismatch and are thus difficult to synthesize by simple approaches. In addition, such structures with high photometric properties have not been reported yet.

Following second approach, solid-solid mixture of Mn and Cu doped core-shell QDs was formed and the system was again exited at 300 nm wavelength (Table SI, Ref. 24). The resultant emission is shown in Figure 7. The recorded emission is similar to one theoretically predicted in Figure 5. The PL spectrum of mixture of Cu doped core-shell QDs and Mn doped core-shell QDs spanning whole spectrum is shown in Figure 7. It is clear that the emission spectrum peaks can be controlled by changing the concentration ratio of Mn and Cu doped QDs. The reabsorption of emitted light is a serious loss mechanism in practical situations. Mn based phosphors that also exhibit high stability and quantum efficiency do not suffer from this problem but in turn lack emission tunability, seriously affecting their practical utility. Hazarika *et al.*[32] addressed this problem by using strain to tune the dopant related emission. We presented a simple way to tune the output spectrum using non-toxic QDs emitting in different parts of visible spectrum at similar excitation. In Figure 7(a), the emission peaks are proportional to each other, while in Figure 7(b) as we increase the concentration of Mn doped core-shell QDs (samples S3 and S4, Table SI, Ref. 24); the peak around red emission is enhanced corresponding to increased concentration of ZnS:Mn/ZnS core-shell QDs. The effect of different concentrations of Cu and Mn doped core-shell QDs on the PL spectrum was studied for all the samples and excitation and emission spectrum of mixture was recorded. The results are summarized in Figure S3 (Ref. 24).

D. Photometric properties

Since QDs are promising color conversion phosphors for lighting and opto-electronic applications, they must have high CRI values with CIE close to white light (0.33, 0.33). Further to generate the warm and stable white color with QDs, the whole visible spectrum must be spanned. The photometric properties (CIE, CCT, and CRI) of 17 samples with various ratios of Cu and Mn doped core shell QDs were studied and their results are depicted in Tables SI and SII (Ref. 24).
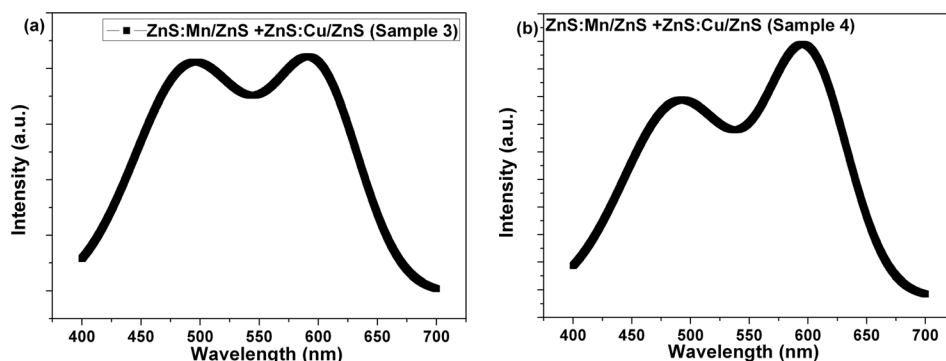

FIG. 7. (a) The PL spectrum of mixture of ZnS:Cu/ZnS and ZnS:Mn/ZnS QD samples spanning the whole spectrum, (b) the peak in red region of spectrum is enhanced as the concentration of Mn is increased (sample S4).

TABLE I. Photometric properties of all types of QDs.

S. no.	QD type	CIE (X,Y)	CCT (in K)	CRI
1	ZnS:Mn	0.49, 0.45	2515	19
2	ZnS:Mn/ZnS	0.48, 0.43	2599	21
3	ZnS:Cu	0.32, 0.43	6111	65
4	ZnS:Cu/ZnS	0.31, 0.41	6109	73
5	ZnS:Mn/ZnS +ZnS:Cu/ZnS (sample S3)	0.33, 0.36	5290	88
6	ZnS:Mn/ZnS +ZnS:Cu/ZnS (sample S4)	0.35, 0.36	4704	88
7	ZnS:Mn/ZnS:Cu	0.48, 0.39	2217	38

On the other hand, Table I summarizes all photometric properties (CIE, CCT, and CRI) of the different types of core-shell QDs. It is clear from Table I that the CRI values increases significantly from 38% to 88% for dual doped sample and mixture of different doped samples (samples S3 and S4), respectively. This increase in CRI happens when the whole spectrum was covered by the emission from the QDs (ZnS:Mn/ZnS + ZnS:Cu/ZnS, sample S4) shown in

Figure 7(b). Only ZnS: Mn QDs have low CRI, which increases as a shell is formed, with a slight shift in CIE co-ordinates ($\Delta x = 0.01$, $\Delta y = 0.02$) as the size of nanoparticle changes after formation of shell, thereby changing the emission. Further, it is seen that CRI value of 38% for dual doped system (ZnS:Mn/ZnS:Cu QDs) is poor because of low emission in 350–550 nm region compared with 550–700 nm region. Thus, the resultant white light is not of very good quality that is needed for solid-state lighting devices. However, when solid–solid mixing of samples was done, the emission of both QDs together spans whole of the visible spectrum, resulting in high value of CRI ~ 88 (Table SII, Ref. 24). Different samples with various ratios of Cu doped and Mn doped QDs were formed as depicted in Table SI. It is found that as the Mn doped ratio of QDs was increased the emission in orange red region of spectrum was enhanced compared with that in blue region (Figure S3, Ref. 24). Further the photometric properties of different samples are depicted in Table I and Table SII. With increase in concentration of Mn doped QDs emission in red region is
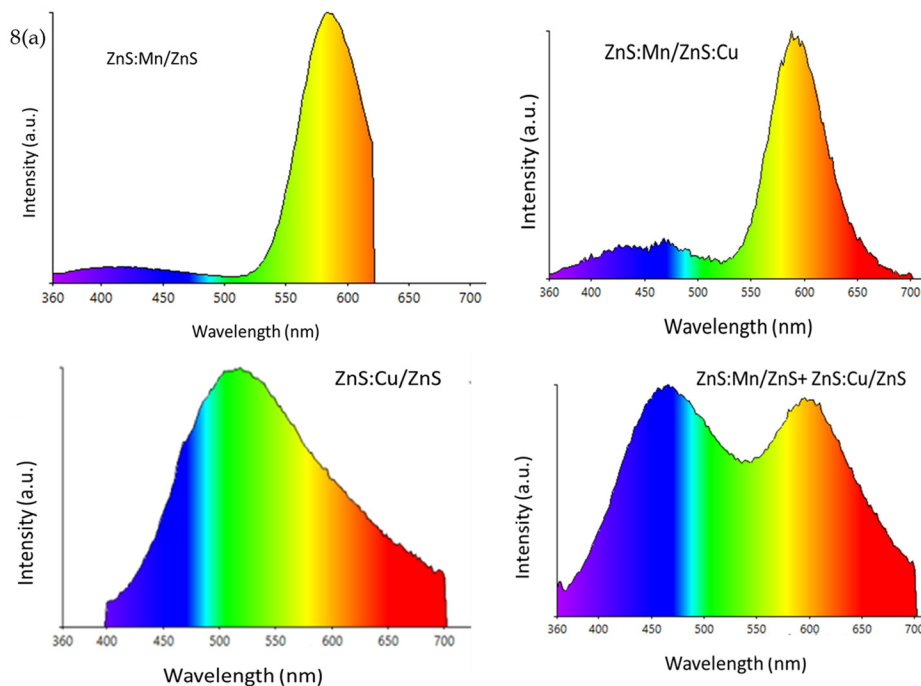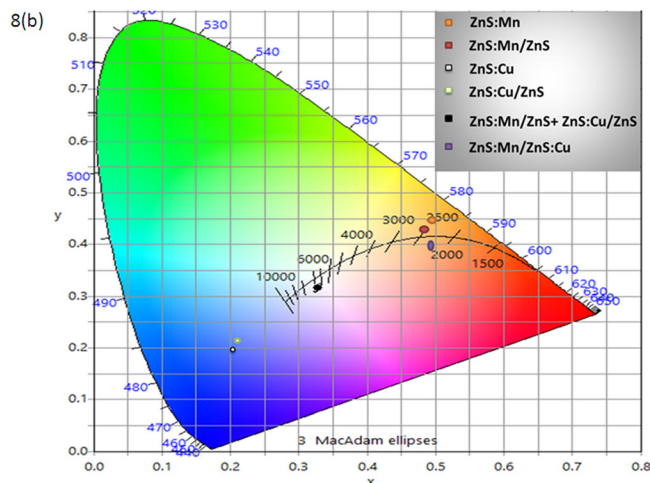

FIG. 8. (a) Emission spectrum spanned by different samples prepared, (b) CIE (x, y) chromaticity diagram of all the nano luminophores prepared.

increased (samples 3 and 4) and the CCT becomes less in comparison to other samples as shown in Table SII. In addition, there is a shift in CIE co-ordinates as well from (0.52, 0.40) to (0.33, 0.36) with an increase in relative concentration of Mn doped QDs with respect to Cu doped QDs. At the same time, if emission in blue region in comparison with red region decreases, the CRI and color (white) quality also decreases. So there is always a tradeoff between CCT and CIE co-ordinates and balance between both of them by adjusting the synthesis and architecture of the system must be achieved. It was observed that the excitation of both the samples was same, but they emit in different region, so it was possible for combining emissions to span the whole visible spectrum. Figure 8(a) shows the spectrum spanned by different samples. It is clear from the figure that sample S3 spans whole visible spectrum. Figure 8(b) depicts CIE (x, y) chromaticity diagram of all inorganic nano fluorophores combinations. The dark line represents black body line at different temperature. It is clear from the diagram that the mixture of Mn and Cu doped QDs can generate warm white light with CIE (0.35,0.36), CRI 88, and CCT 4704 K, which indicates that they can be used to develop QD based white LEDs.

IV. CONCLUSION

In conclusion, we present non cadmium based QD system which can act as a building block for a complete luminescent system needed for potential lighting applications. Different solid-solid mixture of highly luminescent QDs emitting in blue-green and orange region separately were designed to emit white light of good quality under single excitation. The reabsorption problem of mixture (different sized QDs) was successfully addressed since both systems have same excitation and emits differently across the visible spectrum. The resultant mixture have achieved high CRI, however the CCT is a little high in comparison with perfect white light. The CCT of resultant system can be lowered if the emission in the red part of spectrum is further enhanced compared with that of blue green region. The white light emitting system of mixed QDs may lead to a simple device incorporation and improve the overall performance of future solid-state lighting devices. In addition, these doped QDs are safe compared with any of the highly toxic class-A elements (Cd, Hg, and Pb) and may replace the current intrinsic quantum dot emitters used in display and lighting devices.

ACKNOWLEDGMENTS

[1]M. M. Duvenhage, O. M. Ntwaeaborwa, H. C. Swart, and M. J. H. Hoffman, NSTI- Nanotech. **1**, 543 (2010).

[2]M. Chattopadhyay, P. Kumbhakar, C. S. Tiwary, R. Sarkar, A. K. Mitra, and U. Chatterjee, J. Appl. Phys. **105**, 024313 (2009).

[3]Q. Xiao and C. Xiao, Appl. Surf. Sci. **254**, 6432 (2008).

[4]R. Sarkar, C. S. Tiwari, P. Kumbhakar, S. Basu, and A. K. Mitra, Physica E **40**, 3115 (2008).

[5]R. Kripal, A. K. Gupta, S. K. Mishra, R. K. Srivastava, A. C. Pandey, and S. G. Prakash, Spectrochim. Acta, Part A **76**, 523 (2010).

[6]T. T. Q. Hoa, N. D. The, S. McVitie, N. H. Nam, L. V. Vu, T. D. Canh, and N. N. Long, Opt. Mater. **33**, 308 (2011).

[7]B. Dong, L. Cao, G. Sua, and W. Liu, J. Colloid Interface Sci. **367**, 178 (2012).

[8]L. Cao, J. Zhang, S. Ren, and S. Huang, Appl. Phys. Lett. **80**, 4300 (2002).

[9]T. Kubo, T. Isobe, and M. Senna, J. Lumin. **99**, 39 (2002).

[10]A. Kitai, *Luminescent Materials and Applications* (John Wiley & Sons, 2008).

[11]S. Jana, B. B. Srivastava, and N. Pradhan, J. Phys. Chem. Lett. **2**, 1747 (2011).

[12]A. K. Kole, C. S. Tiwary, and P. Kumbhakar, J. Appl. Phys. **113**, 114308 (2013).

[13]S. Murano, M. Burghart, J. Birnstock *et al.*, Proc. SPIE **5937**, 79 (2005).

[14]S. C. Erwin, L. Zu, M. I. Haftel, A. L. Efros, T. A. Kennedy, and D. J. Norris, Nature **436**, 91 (2005).

[15]A. Nag and D. D. Sharma, J. Phys. Chem. C **111**, 13641 (2007).

[16]M. J. Bowers II, J. R. McBride, and S. J. Rosenthal, J. Am. Chem. Soc. **127**, 15378 (2005).

[17]C. C. Shen and W. L. Tseng, Inorg. Chem. **48**, 8689 (2009).

[18]A. A. Bol and A. Meijerink, Phys. Chem. Chem. Phys. **3**, 2105 (2001).

[19]K. W. Cheah, L. Ling, and X. Huang, Nanotechnology **13**, 238 (2002).

[20]S. K. Panda, S. G. Hickey, H. V. Demir, and A. Eychmuller, Angew. Chem. **123**, 4524–4528 (2011).

[21]Z. Quan, D. Yang, C. Li, D. Kong, P. Yang, Z. Cheng, and J. Lin, Langmuir **25**, 10259 (2009).

[22]B. W. D. Andrade, M. E. Thompson, and S. R. Forrest, Adv. Mater. **14**, 147 (2002).

[23]M. Sharma, T. Jain, S. Singh, and O. P. Pandey, AIP Adv. **2**, 012183 (2012).

[24]See supplementary material at http://dx.doi.org/10.1063/1.4927482 for XRD, band gap, luminescence studies, and Tables SI, SII, and SIII.

[25]Powder diffraction File, No. 77–2100 JCPDS International Center for Diffraction Data, 1982.

[26]J. I. Pankove, *Optical Processes in Semiconductors* (Prentice-Hall, Englewood Cliffs, NJ, 1971).

[27]M. Sharma, S. Singh, and O. P. Pandey, J. Appl. Phys. **107**, 104319 (2010).

[28]V. K. Sharma, B. Guzelturk, T. Erdem, Y. Kelestemur, and H. V. Demir, ACS Appl. Mater. Interfaces **6**, 3654 (2014).

[29]R. N. Bhargava, J. Lumin.**70**, 85 (1996).

[30]K. T. Al-Rasoul, N. K. Abbas, and Z. J. Shanan, Int. J. Electrochem. Sci. **8**, 5594 (2013).

[31]R. Sreeja, K. Sridharan, R. Philip, and M. K. Jayaraj, Opt. Mater. **36**, 861 (2014).

[32]A. Hazarika, A. Pandey, and D. D. Sarma, J. Phys. Chem. Lett. **5**, 2208 (2014).

[33]R. B. Little, M. A. EI-Sayed, G. W. Bryant, and S. J. Burke, Chem. Phys. **114**, 1813 (2001).

[34]J. J. Li, A. Wang, W. Guo, J. C. Keay, T. D. Mishima, M. B. Johnson, and X. Peng, J. Am. Chem. Soc. **125**, 12567 (2003).